Distribution Agreement

In presenting this thesis as a partial fulfillment of the requirements for a degree from Emory University, I hereby grant Emory University and its agents the non-exclusive license to archive, make accessible, and display my thesis in whole or in part in all forms of media, now or hereafter now, including display on the World Wide Web. I understand that I may select some access restrictions as part of the online submission of this thesis. I retain all ownership rights to the copyright of this thesis. I also retain the right to use in future works (such as articles or books) all or part of this thesis.

Christian A. Husbands April 10, 2023

Analysis of Factors Required for *Centrocortin* mRNA Localization to Centrosomes in Drosophila Embryos

by

Christian A. Husbands

Dorothy A. Lerit, PhD

Advisor

Biology

Dorothy A. Lerit, PhD

Advisor

Victor Faundez, MD, PhD

Committee Member

Kenneth H. Moberg, PhD

Committee Member

2023

Analysis of Factors Required for *Centrocortin* mRNA Localization to Centrosomes in Drosophila Embryos

By

Christian A. Husbands

Dr. Dorothy A. Lerit

Advisor

An abstract of

a thesis submitted to the Faculty of Emory College of Arts and Sciences

of Emory University in partial fulfillment

of the requirements of the degree of

Bachelor of Science with Honors

Biology

2023

Abstract

Analysis of Factors Required for *Centrocortin* mRNA Localization to Centrosomes in Drosophila Embryos

By Christian A. Husbands

Centrosomes are highly organized and dynamic organelles that serve as the primary microtubule organizing center in animal cells, playing a key role in ensuring proper cell division. Within centrosomes, a compartmentalized matrix of protein and RNA, known as the pericentriolar material (PCM), surrounds a pair of centrioles. Centrosomes function in a multitude of roles throughout the cell cycle, including intracellular trafficking, spindle assembly, and polarization. Recent work from our group demonstrates mRNA localizes to the PCM and contributes to centrosome function, raising the possibility of post-transcriptional links between centrosome dysfunction and disease. One of these centrosomal localizing mRNAs within syncytial *Drosophila* embryos, *Centrocortin* (*cen*), is significantly enriched at the centrosome, where it is organized into micron-scale ribonucleoprotein (RNP) granules. Moreover, *cen* mRNA mislocalization disrupts microtubule organization, leading to impaired nuclear division, increased nuclear fallout, and embryonic lethality. While local *cen* mRNA is required for centrosome function, precisely how *cen* mRNA is targeted to centrosomes remains incompletely understood. Thus, we are investigating the contribution of the minus-end directed dynein motor complex and associated regulatory cofactors to *cen* mRNA localization to centrosomes. We additionally reason that one or more specific sequences within the *cen* gene are responsible for localization. Prior work, for example, suggests *cen* translation is required for *cen* mRNA localization to centrosomes, given that *cen* mRNA and *cen* protein colocalize within *cen* RNPs at the centrosome and *cen* mRNA localization is impaired upon translation inhibition. We are investigating this model and identifying *cis*-elements within the *cen* coding region important for *cen* mRNA localization to centrosomes. This thesis aims to identify possible factors imperative for *cen* centrosomal localization, aspects of which may be impaired in models of centrosomal disease and dysfunction.

Analysis of Factors Required for *Centrocortin* mRNA Localization to Centrosomes in Drosophila Embryos

By

Christian A. Husbands

Dr. Dorothy A. Lerit

Advisor

A thesis submitted to the Faculty of Emory College of Arts and Sciences

of Emory University in partial fulfillment

of the requirements of the degree of

Bachelor of Science with Honors

Biology

2023

Acknowledgements

I would first like to extend my utmost gratitude to my advisor, Dr. Dorothy Lerit, for providing me with the opportunity to explore this sector of biological science that has greatly shaped my undergraduate experience. I would also like to thank Dr. Hala Zein-Sabatto for providing critical guidance throughout the course of this thesis. Additionally, I extend thanks to Jovan Brockett, Lauren Lym, and all other members of the Lerit Lab, past and current, for their added scientific instruction. Finally, I would like to acknowledge Dr. Victor Faundez and Dr. Kenneth Moberg for serving on my thesis committee.

Table of Contents

Introduction

Centrosomes are highly organized and dynamic organelles that function as the primary microtubule organizing center in animal cells. They play key roles in critical cell cycle processes, including intracellular trafficking, spindle assembly, and polarization (Rappaport, 1961). Within centrosomes, a dynamic ring-like matrix of proteins and mRNA known as the pericentriolar material (PCM), surrounds a pair of centrioles (Figure 1; Woodruff et al., 2017). The PCM acts as a platform for protein complexes that regulate centrosomal function by brokering cell cycle regulation, molecule signaling, and microtubule organization (Woodruff et al., 2014). As such, centrosomal dysfunction is implicated in numerous diseases, such as microcephaly, cancer, polycystic kidney disease, and cancer (Dionne et al., 2018).

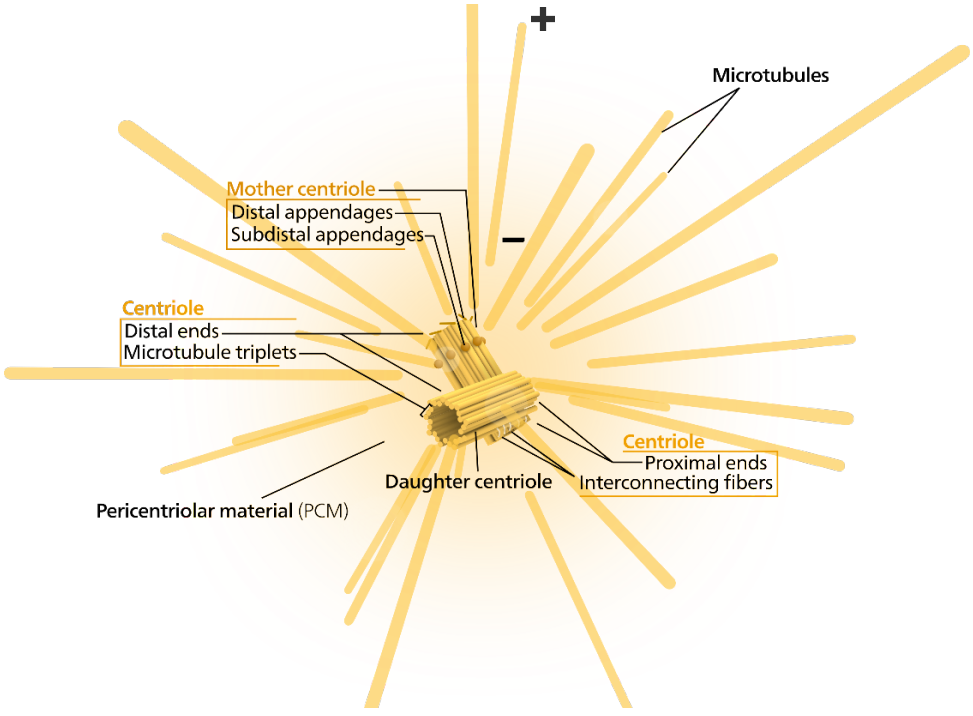

Figure 1. Diagram of Centrosome structure. Diagram illustrating the structure of centrosomes, which are comprised of a pair of centrioles surrounded by the pericentriolar material (PCM). Visualization of minus ends embedded within the PCM along with plus ends facing the cytoplasm (Adapted from Kelvinsong, 2012).

However, the role of centrosomal-localizing mRNA, as it relates to centrosome function via the PCM, has remained less understood. Universally, the localization of mRNA is known to play a critical role in cellular processes and is heavily conserved across eukaryotic and prokaryotic cells. The localization of mRNA serves as a fundamental archetype to define cellular compartments and organelles, akin to the centrosome. Furthermore, being that a small number of mRNA transcripts can regulate large-scale gene expression, the cost-effective nature of mRNA localization makes it an incredibly efficient cellular tool (Figure 2; Martin and Ephrussi, 2009; Zein-Sabatto and Lerit, 2021). Accurate localization of mRNA typically requires the assistance of specific sequence or structural elements in the localizing mRNA termed *cis*-elements. These elements act as "zipcodes", essentially directing the fate of mRNA localization (Eliscovich et al., 2013). In addition, by serving as binding sites for trans-elements that regulate motor protein recognition, for example, cis-element sequences within the mRNA transcript become imperative for proper localization (Zhang et al., 2022). With the efficiency and specificity of active transport, mRNAs are able to localize dynamically to cellular compartments (Figure 2; Martin and Ephrussi, 2009). Thus, defining a mechanism for centrosomal mRNA localization becomes imperative to furthering our understanding of centrosomes as well as mRNA localization.

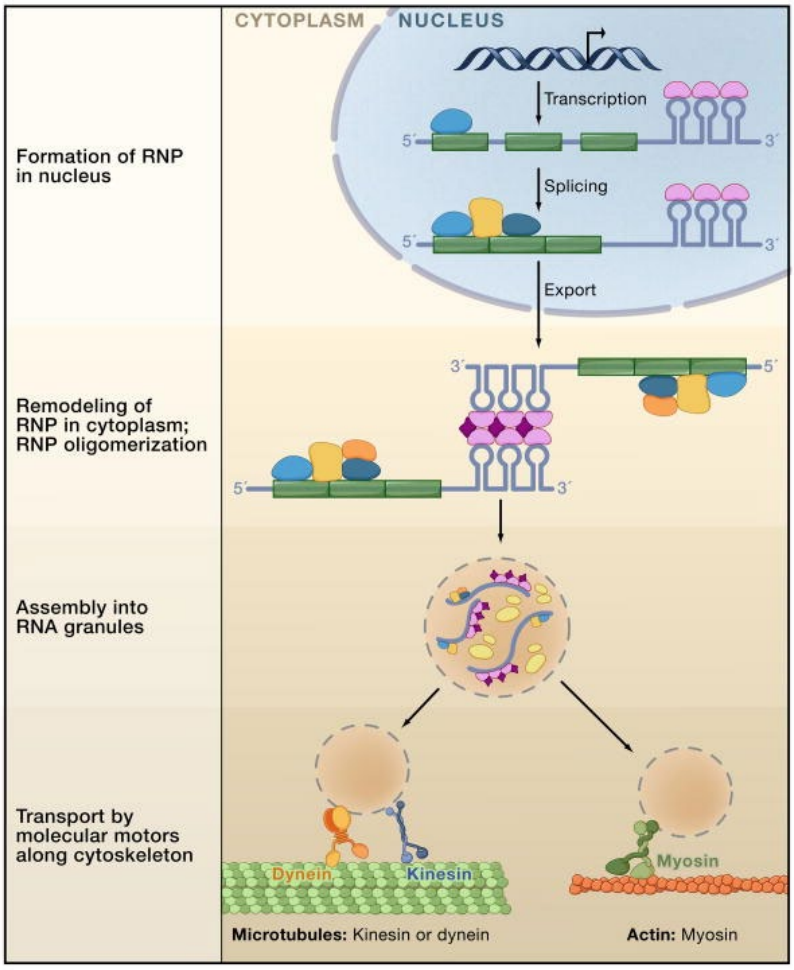

Figure 2. Diagram of the multistep process of mRNA localization. After processing of mRNA transcripts in the nucleus, processed mRNA moves to the cytoplasm and forms into RNA (or RNP) granules. Active transport of these RNP granules along cellular structures allows for targeted localization (Adapted from Martin and Ephrussi, 2009).

Nonetheless, further understanding of localizing mRNAs, as they relate to the PCM, remains a fruitful avenue for the field of cell biology. Long-established experimentation has shown the centrosome's propensity to initiate and regulate poles of bipolar mitotic spindle that ensure proper cell division, genome stability, and formation of daughter cells (Rappaport, 1961). Additionally, high-resolution fluorescent in situ hybridization (FISH) screening has identified a cohort of mRNAs, across numerous cellular compartments, that are present during early *Drosophila* embryogenesis and localize to the centrosome in distinct patterns (Lécuyer et al.,

2007). However, the subcellular factors that govern the localization of these mRNAs to centrosomes remain less understood. Consequently, investigation into the localizing mechanisms of these mRNAs will presumably bolster our understanding of centrosome regulation as it relates to disease and dysfunction.

One of the centrosomal localizing mRNAs identified within syncytial *Drosophila* embryos, *Centrocortin* (*cen*), was previously demonstrated by our laboratory to be significantly enriched at the centrosome, organizing into micron-scale ribonucleoprotein granules (RNPs) that contain *cen* mRNA and protein (Ryder et al., 2020). Localization of *cen* peaks during interphase at nuclear cycle (NC) 13, the stage at which embryos endure a prolonged interphase (Foe and Alberts, 1983; Ryder et al., 2020). Our group mislocalized *cen* mRNA by generating chimeric *cen-bcd-3' UTR* embryos to examine whether loss of *cen* localization to centrosomes altered centrosome functions. For these experiments, the *cen* coding sequence was fused to the *bicoid* (*bcd*) 3' UTR, previously shown to be sufficient to target reporter RNAs to the anterior pole (Macdonald and Struhl, 1988). As predicted, *cen-bcd-3' UTR* embryos generated an anterior crescent of *cen* mRNA during syncytial development. Additionally, during the progression of the cell cycle, *cen* mRNA mislocalization disrupted nuclear divisions due to microtubule disorganization and increased nuclear fallout, which culminated in embryonic lethality (Ryder et al., 2020). As such, when taking these findings into consideration along with defined modes of mRNA localization (Figure 2), the possibility of *cen* mRNA localization utilizing active transport for centrosome targeting becomes apparent.

As we consider the possibility of *cen* mRNA localization utilizing active transport, it is known that microtubules nucleated by the centrosome are characterized by their distinct minus and plus ends (Figure 1). Their polarized nature arises from fact that their structure is comprised

of alpha- and beta-tubulin heterodimers (Goodson and Jonasson, 2018). Being that microtubules polymerize from the plus ends facing the cytoplasm, the minus ends are embedded within the γ-tubulin ring complex (γTURC) of the PCM (Figure 1; Moritz et al., 1995). Microtubules bear responsibility for critical cellular functions, such as intracellular transport, which uses cytoplasmic dynein and kinesin motor proteins to travel along the polarized microtubules in the minus- or plus-end directions, respectively (Ross et al., 2008; Xiang and Qiu, 2020). Thus, we hypothesize that mRNAs residing at the centrosome may require dynein-mediated transport for efficient localization.

Preliminary data from Dr. Simon Bullock's lab at MRC labs in the United Kingdom reinforces suspicions for dynein's involvement in *cen* mRNA localization. The presence of a highly conserved dynein light intermediate chain (DLIC) sequence was identified within the *cen* coding sequence by bioinformatics (Figure 3). Furthermore, a biochemical interaction between Cen and the DLIC was confirmed by immunoprecipitation (Figure 4). Thus, our first postulate revolves around the possibility of the minus-end directed dynein motor complex contributing to the regulation of centrosomal mRNA localization.

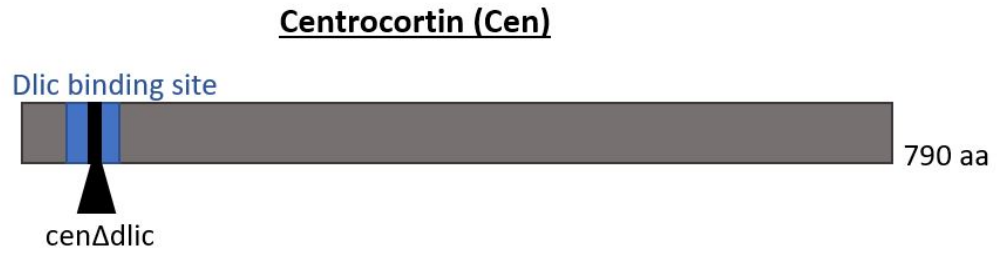

Figure 3. *Centrocortin* coding sequence contains a conserved dynein light intermediate chain (DLIC) binding region. The *Centrocortin* sequence contains a conserved DLIC binding site, confirmed by bioinformatics (Dr. Simon Bullock, Unpublished).

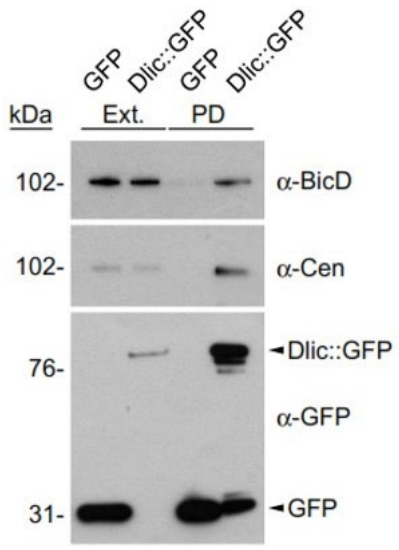

Figure 4. Immunoprecipitation of Centrocortin protein via dynein light intermediate chain (DLIC). From left to right, in the 3rd and 5th lanes, we are able to see the presence of Cen protein using DLIC::GFP, but not GFP alone. This provides evidence for an interaction between Cen and the DLIC (Dr. Simon Bullock, Unpublished).

Furthermore, we and others showed *cen* RNPs contain both *cen* mRNA and *cen* protein, which coalesce during the early stages of *Drosophila* embryogenesis in a cell cycle dependent manner (Bergalet et al., 2020; Ryder et al., 2020). In *cen-bcd-3' UTR* embryos, *cen* mRNA failed to localize to more distal centrosomes. Notably, Cen protein and *cen* mRNA were also absent at distal centrosomes, demonstrating the localization of *cen* mRNA and protein is coupled and that *cen* mRNA is sufficient and necessary for centrosome targeting (Ryder et al., 2020).

Others were also able to show that *cen* mRNA was sufficient for centrosome targeting through an interdependency analysis of co-localizing centrosomal *cen* and *ik2* mRNAs (Bergalet et al., 2020). It was found that the localization of *ik2* mRNA to the centrosome was dependent on *cen* mRNA, evident from FISH imaging in *cen*-deficient mutants. However, when analyzing centrosomal localization patterns in *ik2* RNAi mutants, the localization of *cen* mRNA was unaffected (Bergalet et al., 2020). Moreover, by use of a puromycin proximity ligation assay

(Puro-PLA) to disrupt Cen protein synthesis, it was shown that *cen* mRNA undergoes localized protein synthesis when in proximity to centrosomes (Bergalet et al., 2020). These results collectively raise questions regarding *cen* mRNA translation being necessary for *cen* mRNA localization.

We also demonstrated *cen* RNPs incorporate a translational repressor, the conserved RNA-binding protein fragile X mental retardation protein (FMRP). Depletion of FMR1, the gene encoding for FMRP, led to increased localization of *cen* mRNA to centrosomes and elevated levels of Cen protein, further suggesting a regulatory link between *cen* mRNA translation and *cen* mRNA localization (Ryder et al., 2020). Nevertheless, the requisites of *cen* mRNA localization to centrosomes remain largely unknown. As such, our second postulate revolves around the possibility that the translation of one or more specific *cis*-element sequences within the *cen* protein coding sequence are critical for *cen* mRNA localization.

Beginning the investigation regarding our first postulate of the minus-end directed dynein motor complex bearing significance for the regulation of *cen* mRNA localization, we first identified embryonically viable dynein heavy chain (*Dhc*) mutation combinations in *Drosophila*. The first *Dhc* mutation interrogated was $Dhc64C^{loa}$ (Legs at odd angles; LOA), a dominant loss-of-function F580Y point mutation in the dynein heavy chain that has been reported to invoke the decimation of motor neurons in mice (Ilieva et al., 2008; Deng et al., 2010). However, embryo production of homozygote combinations of LOA *Drosophila* lines was diminutive. In response to this, we examined *Dhc64C* hemizygotes that contained LOA and a TM6C balancer chromosome, genotype LOA/+. To further compromise dynein function, we identified a second *Dhc64C* mutation, $Dhc64C^{8\text{-}1}$ (8-1), a recessive hypomorphic mutation governing cell viability in several *Drosophila* tissues that, in combination with LOA, produced a viable number of embryos

for analysis (Gepner et al., 1996). To evaluate the significance of the dynein motor complex for *cen* mRNA localization, we compared the *cen* mRNA localization patterns between control, LOA/TM6C hemizygotes, and LOA/8-1 transheterozygous mutants. Further assessment of homozygote *Dhc* mutants is likely necessary to more accurately appraise the significance of the minus-end directed dynein motor complex as it relates to *cen* mRNA localization.

Next, to address our second postulate that the translation of one or more specific sequences within the *cen* protein coding sequence are critical for *cen* mRNA localization, we created two differing transgenic *Drosophila* lines using the power of Gibson Assembly (Gibson et al., 2009). The first transgenic line was assembled using an unmodified *cen* coding DNA (cDNA) sequence that was flanked with a C-terminal hemagglutinin (HA) tag added to detect expression via anti-HA antibodies in immunofluorescence or western blotting. The second transgenic line was assembled using a *cen* cDNA sequence that lacked the translation-initiating start codon and was also flanked by an identical C-terminal HA tag. Cloning procedures for each transgenic line were successful and developed viable transgenic *Drosophila* lines, however, the resulting lines were not able to be received from the commercial vendor (BestGene, Inc.) in time for analysis in this thesis. Further investigation into *cen* mRNA localization pattern of each line would prove promising for future study.

Results

Significance of the minus-end directed dynein motor complex for cen mRNA localization

On the significance of the minus-end directed dynein motor complex, we hypothesize that this complex is imperative for *cen* mRNA localization to the centrosome. As previously discussed, *cen* mRNA localizes to the centrosome dynamically throughout the cell cycle. Furthermore, mislocalization of *cen* mRNA via *cen-bcd-3' UTR* mutants leads to disrupted nuclear division, nuclear fallout, and microtubule disorganization (Ryder et al., 2020). Additionally, given that cytoplasmic dynein-mediated transport has been shown to be minus-end directed (Ross et al., 2008; Xiang and Qiu, 2020) and the minus-ends of microtubules are incorporated within the γ-tubulin ring complex (γTURC) of the PCM (Moritz et al., 1995), we used genetic analysis to test the importance of dynein for *cen* mRNA localization.

Dr. Simon Bullock's lab provided novel CRISPR mutants that disrupted a conserved DLIC binding site within the N-terminus of the *cen* coding sequence, which resulted in a significant reduction in *cen* mRNA localization to centrosomes (Figure 5). We employed single molecule FISH (smFISH) to visualize endogenous *cen* mRNA localization and further quantified the extent of *cen* mRNA localization to centrosomes using a custom computational analysis workflow previously developed by our lab (Ryder and Lerit., 2020). *Cen*Δ12 mutants, consisting of an in-frame mutation that deleted 12 nucleotides of the conserved binding site, showed slightly decreased *cen* mRNA localization as well *cen* RNP granule formation (Figure 5B). However, when disrupting the DLIC binding site with *cen*Δ5 mutants, consisting of an out-of-frame mutation that deleted 5 nucleotides, we saw an obliteration of *cen* mRNA localization and

cen RNP granule formation (Figure 5C). As such, a requirement for the DLIC bolsters our hypothesis that dynein is required for *cen* mRNA localization to centrosomes.

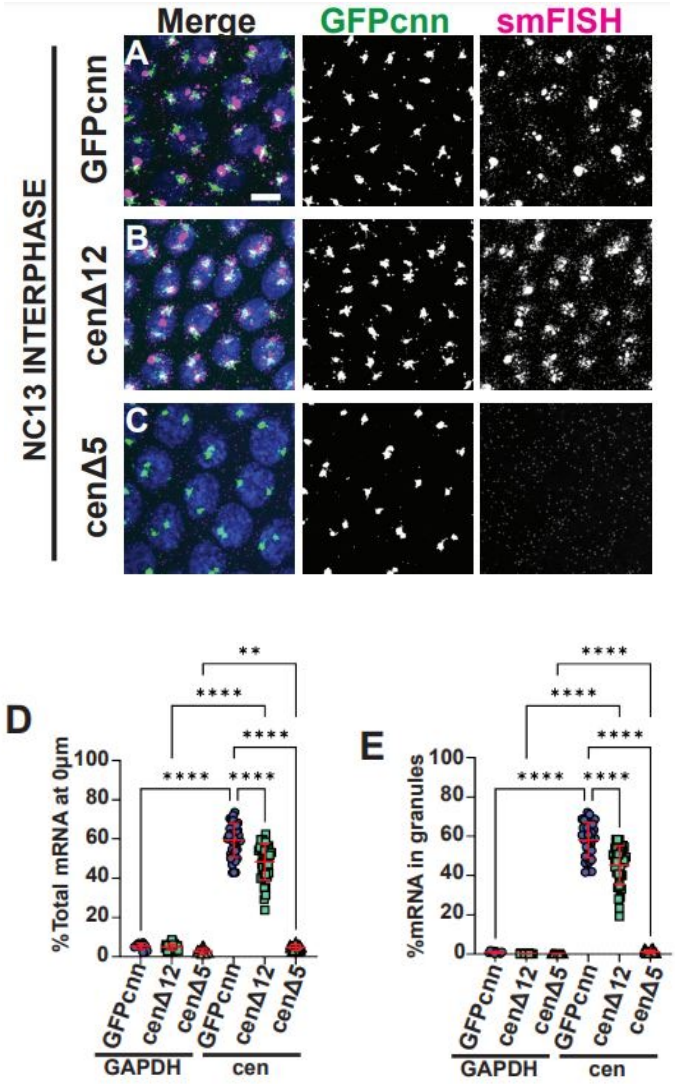

Figure 5. smFISH of *cen* mRNA localization in *cen* CRISPR mutants. Two CRISPR mutants, *cen*Δ12 and *cen*Δ5, containing in-frame and out-of-frame nucleotide deletions that disrupted a conserved DLIC binding site, respectively, show differing *cen* mRNA localization (% total RNA at 0 µm) as well as *cen* RNP granule formation. In *cen*Δ12 mutants, *cen* mRNA localization as well as *cen* RNP granule formation were decreased slightly when compared to the GFPcnn control (B, D, E). In *cen*Δ5 mutants, *cen* mRNA localization as well as *cen* RNP granule formation were completely obliterated (C, D, E). GAPDH serves as a negative control. Embryos imaged at NC 13 interphase. Scale bar (A) represents 5 µm. Statistical analyses were conducted using a Brown-Forsythe and Welch ANOVA followed by Dunnett's T3 multiple comparisons test (*, P<0.05; **, P <0.005; **** P<0.0001). Data represents 3 independent experiments, with total n ≥ 30 for each fly line (Dr. Hala Zein-Sabatto, Unpublished).

To directly test whether dynein contributes to *cen* mRNA localization, our goal was to maternally deplete dynein within embryos and quantify changes to *cen* mRNA localization to centrosomes relative to controls via smFISH. Dynein is required in many cellular and developmental processes, including oogenesis and embryonic axis patterning (Clark et al., 2007). Thus, my postdoctoral fellow mentor, Dr. Hala Zein-Sabatto, first assayed numerous transheterozygous combinations of classic *Dhc64C* alleles to identify those that would yield sufficient embryos for further analysis. The first mutation identified was LOA, a novel *Dhc64C* allele generated by the Bullock lab in *Drosophila*, which is a dominant loss-of-function F580Y point mutation in the dynein heavy chain that disrupts motor neurons (Ilieva et al., 2008; Deng et al., 2010). We initially intended to collect homozygote LOA/LOA embryos, but were unable to collect a sufficient number. As such, we decided to use hemizygote LOA mutants in trans to the TM6C balancer, genotype LOA/+, to collect a sufficient number of embryos for analysis. These *Dhc64C* hemizygotes were predicted to maintain 50% of normal dynein activity. To further investigate the effect of dynein mutations, we enlisted a second *Dhc64C* mutation, termed 8-1, that is a recessive hypomorphic mutation governing cell viability in several *Drosophila* tissues (Gepner et al., 1996). We subsequently collected embryos from LOA/8-1 transheterozygous mutants for analysis. The nature of the dominant loss-of-function LOA and recessive hypomorphic 8-1 mutations were hypothesized to have a dose-dependent deleterious effect based on existing statistical models in conventional genetics (Setu et al. 2021).

To evaluate the distributions of *cen* mRNA localization in control, LOA/TM6C, and LOA/8-1 embryos, we again employed smFISH to visualize and quantify endogenous *cen* mRNA localization in embryos expressing GFP-γTubulin23C (GFP-γTub) to label the centrosomes. Because we previously noted peak *cen* mRNA enrichment at centrosomes at NC

stage 13, we focused our analysis on this stage of syncytial development. Our results suggest that the minus-end directed dynein motor complex does in fact bear significance in relation to the localization of *cen* mRNA as *cen* mRNA localization and RNP granule formation were shown to increase in LOA/TM6C and LOA/8-1 mutants relative to the control (Figure 6).

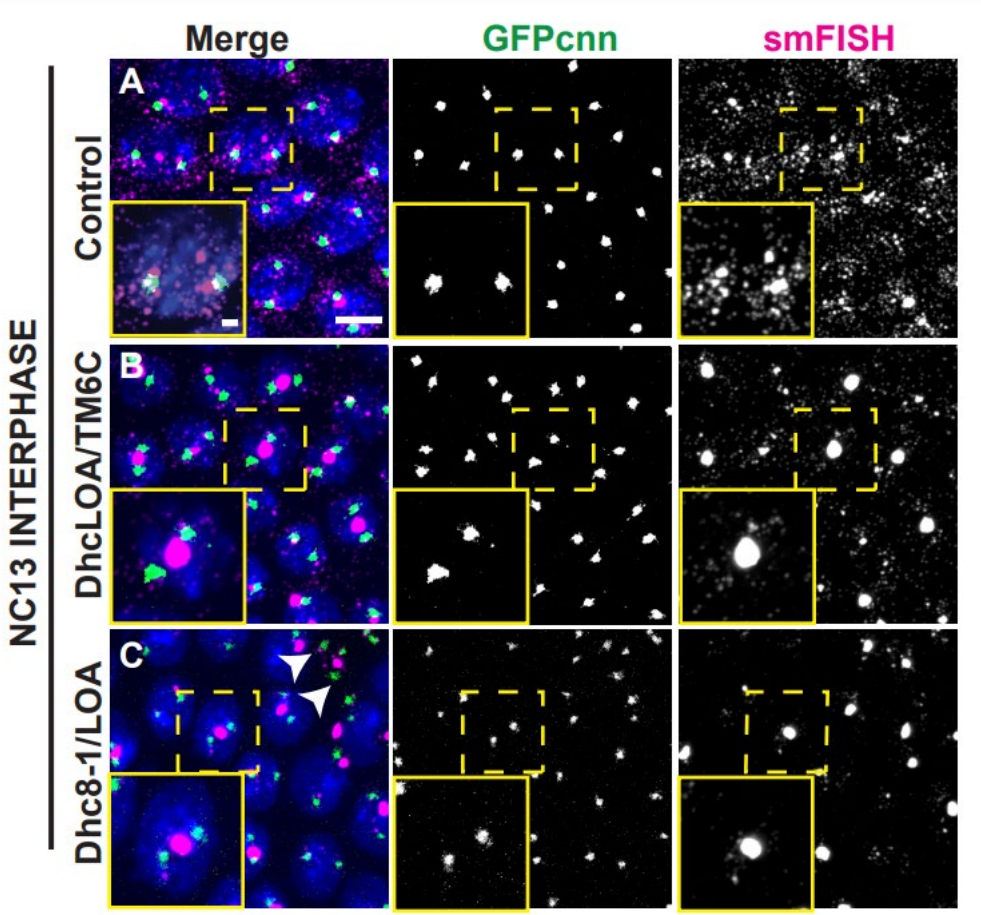

Figure 6. smFISH of *cen* mRNA localization in embryos of GFPcnn control, LOA/TM6C, and LOA/8-1 mutants. *cen* mRNA was detected using smFISH (pink) in embryos expressing GFP-γTubulin23C (GFP-γTub) (green). Nuclei were stained blue with DAPI. LOA/TM6C mutant shows greater formation of *cen* mRNA RNP granules and centrosomal localization compared to the GFPcnn control (B). LOA/8-1 trans-het mutant further shows increased formation of *cen* mRNA RNP granules and centrosomal localization compared to the LOA/TM6C mutant (C). Arrows in C show nuclear detachment phenotype present in several LOA/8-1 mutant embryos. Scale bar (A) represents 5 µm. Inset scale bar (A) represents 1 µm. Embryos were imaged at NC 13 interphase.

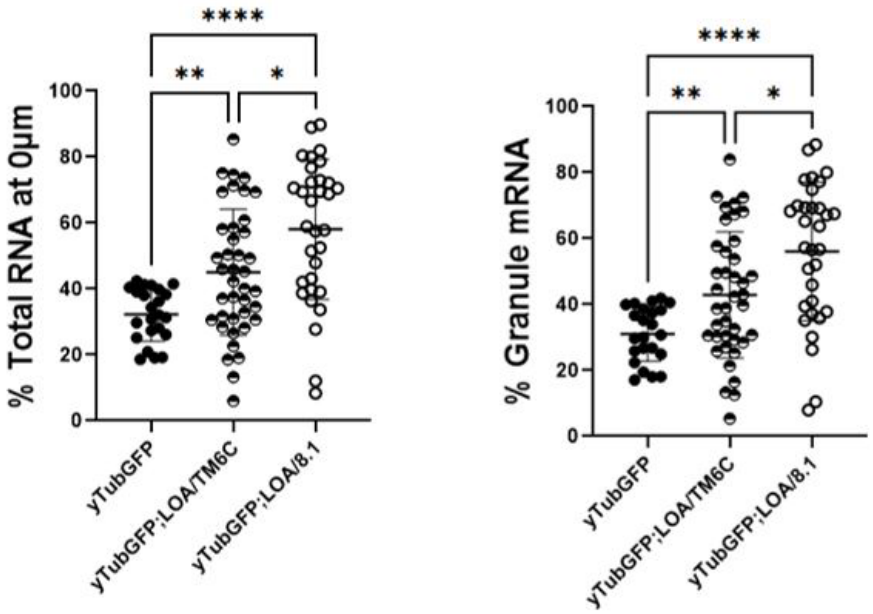

Figure 7. Quantification of *cen* mRNA localization in embryos of GFP-γTub control, LOA/TM6C, and LOA/8-1. *cen* mRNA localization (% total RNA at 0 µm) and granule formation were quantified using GraphPad Prism software and RNA detection measurement procedures. LOA/TM6C mutants show greater formation of *cen* mRNA RNP granules and centrosomal localization compared to GFP-γTub controls. LOA/8-1 trans-het mutants further show increased formation of *cen* mRNA RNP granules and centrosomal localization compared to the LOA/TM6C mutant. Statistical analyses were conducted using a Brown-Forsythe and Welch ANOVA followed by Dunnett's T3 multiple comparisons test (*, $P<0.05$; **, $P<0.005$; **** $P<0.0001$). Data shown are representative results from at least 3 independent experiments. Total $n \geq 30$ for each respective fly line.

Unexpectedly, visualization and quantification revealed significantly increased *cen* mRNA localization at the centrosomes as well has a higher percentage of *cen* mRNA formed into RNP granules within *Dhc* mutants relative to controls (Figures 6 and 7). Furthermore, comparing LOA/TM6C to LOA/8-1 also demonstrated a statistically significant dose-dependent effect on *cen* mRNA localization and *cen* RNP granule formation, consistent with our hypothesis, as the LOA/8-1 combination appeared to be increased in both aspects (Figure 6B, 6C, and 7). We also visualized a recurrent phenotype of nuclear detachment in LOA/8-1 mutants (Figure 6C). While these results do support the hypothesis that the dynein motor complex

regulates *cen* mRNA localization, we originally predicted loss of dynein would reduce, not increase, centrosomal mRNA localization (Figure 10). Further analysis of homozygote mutations will be crucial to gain a clearer understanding of dynein's role in *cen* mRNA localization.

Translational significance of the cen protein coding sequence for cen mRNA localization

We and others uncovered that the *cen* coding sequence is necessary and sufficient to target *cen* mRNA to centrosomes (Bergalet et al., 2020; Ryder et al., 2020). Our prior analysis of *cen-bcd-3'UTR* embryos uncovered centrosomal defects in the absence of both *cen* mRNA and protein. These data raise the possibility that either *cen* mRNA or protein are required for centrosome function. It remains formally possible that *cen* mRNA contributes to centrosome activity. Alternatively, the co-transport and/or local translation of Cen protein may be required for centrosome regulation. Thus, our goal was to devise a strategy to specifically impair Cen translation. Prior work indicates translation inhibitors, such as puromycin, disrupt *cen* mRNA localization (Bergalet et al., 2020). However, such pharmacological approaches lack specificity, which could confound interpretation of resulting phenotypes.

Thus, to test this postulate of translational significance, we designed two distinct transgenic *Drosophila* lines by way of genetic cloning. The first transgenic line contained an unaltered *cen* coding sequence that was flanked by a C-terminal hemagglutinin (HA) tag that could be used for protein detection by immunofluorescence or western blotting via anti-HA antibodies. The second line contained the *cen* coding sequence with the translation initiating start codon (ATG) removed, followed by an identical HA tag (Figure 8). Due to the relatively small size of the *cen* sequence and low number of pieces required for construct generation, we employed Gibson Assembly for genetic cloning.

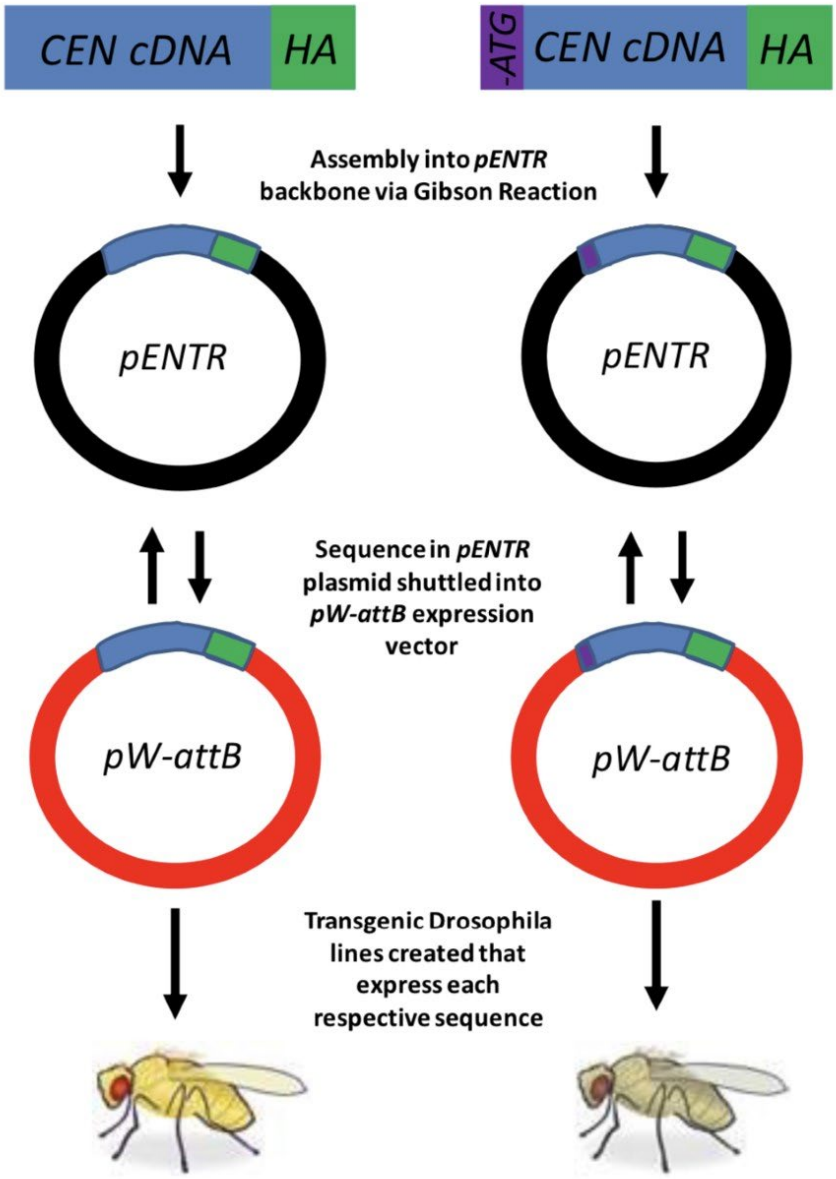

Figure 8. Diagram of *cen* transgenic sequence construction. Transgenic *Drosophila* sequences were created with and without the *cen* translational start codon to test for possibility that translation is imperative for *cen* mRNA localization. Genetic cloning was conducted via Gibson Assembly. Assembled sequences were shuttled into a *pPW-attB* expression vector and were subsequently sent for transgenesis to a commercial vendor (BestGene, Inc.).

To construct the distinct transgenic *cen* lines via Gibson Assembly, we utilized PCR to amplify the pENTR backbone and *cen* coding sequence, each with and without the sticky ends corresponding to the translational start codon. The expected size of the pENTR backbone was 2.6 kilobases (kb) (Figure 9A, 9C, 9B), while the *cen* coding sequence totaled 2.5 kb (Figure 9A, 9D). Amplification was confirmed using a primer negative control that did not that contain a template sequence and was expected to dimerize, yielding a small size (Figure 9A). Once assembled into the pENTR backbone, we shuttled our *cen*-HA fusion sequences into a *pPW-attB Drosophila* expression plasmid via gateway destination (Figure 8). The *pPW-attB* plasmid is defined by the UASp enhancer element (*P*) for germline transmission and expression, the gateway cassette (*W*), and attB sites (*-attB*) for site-specific phi-31C integration into the genome. Isolated expression plasmids were then sent to a commercial vendor (BestGene, Inc.) for *Drosophila* transgenesis and site-specific integration into the attP2 site on chromosome 3. Chromosome 3 was selected due to the cytogenetic location of *cen*, which falls on chromosome 2. Ultimately, we wish to drive expression of *pUASp-cen(+/-ATG)-HA* in the *cen* null background to assay for mRNA localization to centrosomes. Unfortunately, while viable transgenic lines were created (4 independent isolates for -ATG and 5 independent isolates for +ATG), they were not received in time for analysis in this thesis. Further study that focuses on the *cen* mRNA localization pattern of each respective transgenic line remains fruitful for future analyses.

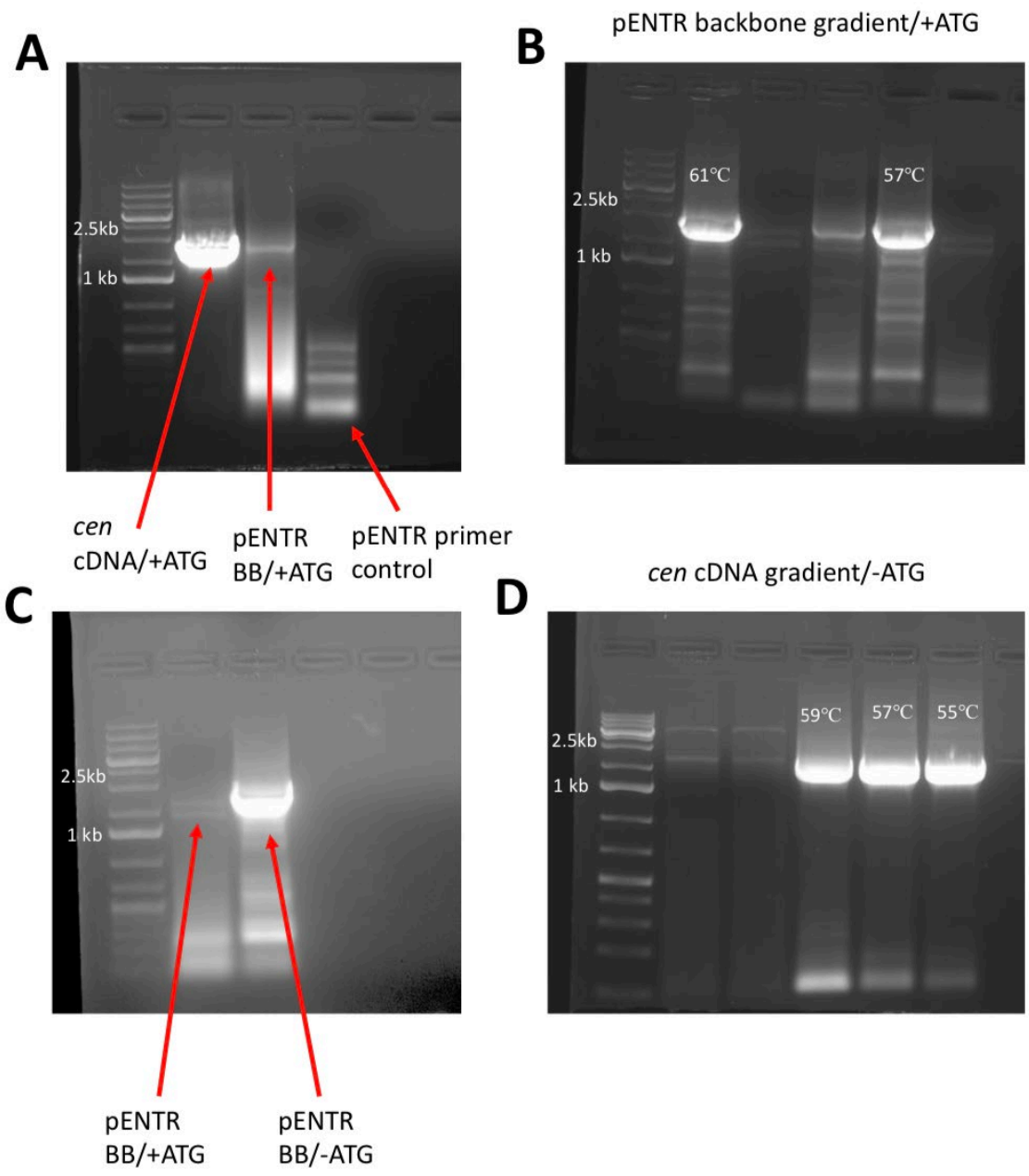

Figure 9. Accumulation of required PCR pieces for Gibson Assembly. Gibson assembly was used to PCR amplify the pENTR backbone and *cen* coding sequence, each with (+) and without (-) the sticky ends corresponding to the translational start codon (ATG). A negative control that did not contain template DNA was used (A). Image shows ethidium bromide-stained DNA agarose gel electrophoresis of amplified pieces with a Thermoscientific GeneRuler 1kb DNA ladder for reference. The expected size of the pENTR backbone was 2.6 kilobases (kb). The expected size of the *cen* coding sequence was 2.5 kb. PCR gradients were used to address trouble with identifying optimal PCR primer annealing temperature for exceptional amplification.

Discussion

In most Eukaryotic cells, the centrosome serves as the primary microtubule organizing center, holding a significant role in many well-defined cellular processes. However, the relationship between mRNA localization and centrosomes remains less understood. Existing research has only just begun to scratch the surface of mRNA localization to centrosomes during the cell cycle. Evidence has arisen that numerous mRNA transcripts, such as *Centrocortin* (*cen*), localize to the centrosome and contribute to centrosomal function (Lécuyer et al., 2007; Ryder et al., 2020). However, the specific mechanism governing how mRNAs localize to the centrosome has remain undefined. As such, this thesis aimed to identify factors required for *cen* mRNA localization to centrosomes in *Drosophila*. We predicted loss of dynein would impair *cen* mRNA localization to centrosomes (Figure 10). However, our data support a model where dynein heavy chain (*Dhc*) mutations, required for intracellular trafficking, unexpectedly increase *cen* mRNA localization and ribonucleoprotein (RNP) granule formation (Figure 11).

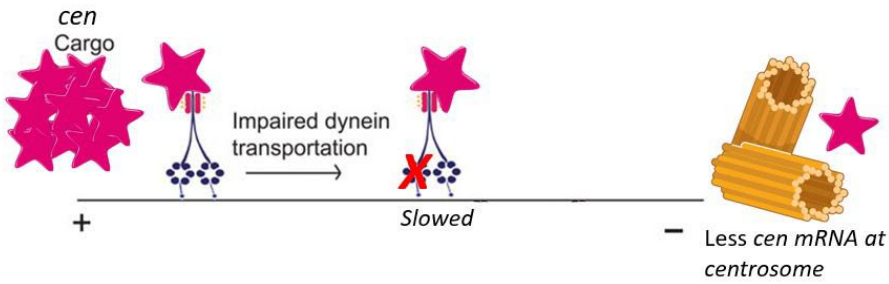

Figure 10. Original model for the effect of the *Dhc* mutations on dynein mediated cargo transport. This cartoon model represents our initial hypothesis for the effect of *Dhc* mutations on dynein mediated cargo transport directed to the minus ends of microtubules embedded in the PCM of centrosomes (Adapted from Deng et al., 2010). We originally hypothesized that *Dhc* mutations would impair dynein transportation and simply slow down transport, leading to decreased amounts of *cen* RNP cargo at the centrosome, given that neither LOA/TM6C hemizygotes or LOA/8-1 transheterozygotes would completely impair dynein function.

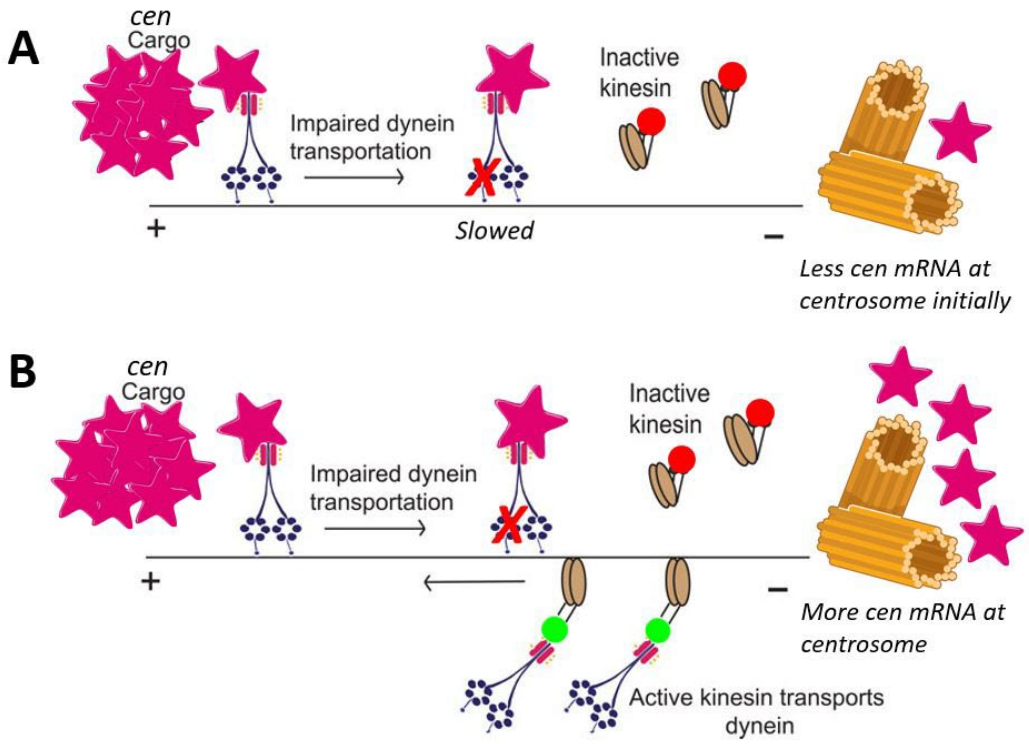

Figure 11. Revised model for the effect of *Dhc* mutations on dynein mediated cargo transport. This cartoon model represents our revised hypothesis for the effect of *Dhc* mutations on dynein mediated cargo transport directed to the minus ends of microtubules embedded in the PCM of centrosomes (Adapted from Deng et al., 2010). Schematic A demonstrates the global response of slow dynein *cen* RNP cargo transportation due to possible cellular responses (red) to *Dhc* mutations that lead to an inactivation of kinesin, preventing anterograde transport of dynein motors. Schematic B demonstrates the local response to this inactivation of kinesin. Local cellular responses (green) lead to the activation of kinesin, increasing anterograde transport of dynein motors, which would in turn increase retrograde *cen* cargo transport towards the centrosome. The local response (green) would presumably be stronger in *Dhc* mutants as compared to GFP-γTub controls, providing an explanation for increased *cen* mRNA at the centrosome due to a higher rate of dynein motor recycling.

To support our original model (Figure 10), we set out to identify embryonically viable *Dhc* mutant combinations to analyze *cen* mRNA centrosomal localization. Two mutant combinations were used for our analysis. The first mutation we attempted to utilize was *Dhc64C*^{loa} (LOA), a dominant loss-of-function F580Y point mutation in the dynein heavy chain

that was shown to lead to the destruction of motor neurons (Ilieva et al., 2008; Deng et al., 2010). However, homozygote combinations of LOA flies were not embryonically viable for analysis. Instead, we decided to utilize LOA/TM6C hemizygotes with the hope that the 50% mutational reduction, due to the introduction of a balancer, would produce a viable number of embryos that could be used for analysis. To further test for the effects of contributing *Dhc* mutations, we identified a second mutation named $Dhc64C^{8\text{-}1}$ (8-1); a recessive hypomorphic mutation governing cell viability in several Drosophila tissues (Gepner et al., 1996). Transheterozygous LOA/8-1 mutants were able to produce a viable number of embryos for analysis.

Our data demonstrated that the localization of *cen* mRNA and *cen* RNP granule formation increased in LOA/TM6C and LOA/8-1 mutants relative to the control (Figure 6, Figure 7). These data force us to reconsider our original model (Figure 10) to account for a mechanism whereby loss of dynein permits increased *cen* mRNA localization to centrosomes (Figure 11). Based on our results, we hypothesize that global cellular factors respond to slow dynein cargo transportation, due to possible cellular responses to *Dhc* mutations, leading to an inactivation of kinesin and preventing anterograde transport of dynein motors (Figure 11A). We further hypothesize that local cellular factors then lead to an increase in kinesin activation as a response to impaired dynein transportation and kinesin inactivation that slows down transport (Figure 11B). By increasing kinesin activation, retrograde transport of *cen* RNP cargo towards the centrosome increases as dynein motors are recycled more quickly to load more anterograde cargo. This assumption also makes sense within the context that neither LOA/TM6C hemizygotes or LOA/8-1 transheterozygotes would completely impair dynein function due to only 50% LOA being present in each, along with 8-1 being a hypomorphic mutation. Further analysis into what cellular factors may be govern potential kinesin activation/inactivation could

serve as a basis for future analysis. Additionally, comparing the local amount of activated kinesin in *Dhc* mutants to control flies would bolster the result. There is also a possibility that other minus-end directed motors play a role in *cen* mRNA transport to the centrosome, given that *Nonclaret disjunctional (Ncd)* in *Drosophila* has been shown to encode a minus-end directed kinesin-14 motor (Ambrose et al., 2005).

To further define the mechanism of *cen* mRNA localization to the centrosome, we also set out to identify *cis*-elements within the *cen* protein coding sequence to evaluate translational significance. The basis for this postulate came from evidence that suggests *cen* mRNA localization is necessary for Cen protein localization to centrosomes (Ryder et al., 2020, Bergalet et al., 2020). To test this, we designed two transgenic HA-tagged constructs of the *cen* protein coding sequence (Figure 8) that could evaluate the importance of translating the entire *cen* protein coding sequence for *cen* mRNA localization via a translational start codon deletion (Figure 9). The inclusion of an HA tag would allow us to independently verify the presence of our transgenic products with the use of anti-HA antibodies in immunofluorescence or western blotting. Unfortunately, while viable transgenic lines were created, they were not received in time for analysis in this thesis. However, based on previously discussed research that shows *cen* mRNA is sufficient for centrosome targeting and co-transports with Cen protein in granules (Ryder et al., 2020; Bergalet et al., 2020) as well as the fact that *cen* mRNA undergoes local translation in proximity to centrosomes in a puromycin proximity ligation assay (Bergalet et al., 2020), we hypothesize that the localization of *cen* mRNA is dependent on the translation of *cen* mRNA, where *cen* mRNA localization will be diffuse without Cen protein. It also remains possible that the localization of *cen* mRNA dependent on the translation of *cen* mRNA and bears more significance to defined mRNA “zipcodes” and RNA binding proteins (Das et al., 2021),

where *cen* mRNA can be localized to centrosomes irrespective of Cen protein. Once received, analysis that focuses on the *cen* mRNA localization pattern of each respective transgenic construct will provide critical insight into the nature of *cen* mRNA localization.

Being able to clearly outline a mechanism of *cen* mRNA localization to the centrosome and its accompanying factors remains crucial to advancing our knowledge of subcellular mRNA localization. Several mRNAs within syncytial Drosophila embryos have been shown to subcellularly localize (Lécuyer et al., 2007). Additionally, mRNA localization is a powerful cellular tool that allows for efficient transport and control of gene expression (Martin and Ephrussi., 2009). As such, it is no surprise that mRNA localization is highly conserved across many subcellular compartments, including the centrosome (Ryder et al., 2020; Zein-Sabatto and Lerit., 2021). The model that we are proposing (Figure 11) portrays differing global and local responses to impaired dynein mediated *cen* cargo transport towards the minus-end of microtubules embedded within the PCM of centrosomes, where kinesin activation plays an active role in continuing transport. Given the commonality and conserved nature of dynein as a cellular motor, it is entirely possible that mutations within its heavy chain complex may lead to many dysfunctions in other subcellular compartments (Deng et al., 2010). Moreover, mislocalizing centrosomal mRNAs, like *cen*, can lead to a myriad of cellular dysfunctions that include microtubular disruption, nuclear fallout, and embryonic lethality (Ryder et al., 2020). These cellular dysfunctions bear even more importance as they are implicated in overarching disease states that include, cancers, polycystic kidney disease, and microcephaly (Dionne et al., 2018). Whether localization of centrosomal RNAs to centrosomes is impaired in diseased cells remains an exciting topic for future study.

Materials and Experimental Procedures

Fly Stocks

The following *Drosophila* lines were used in this study: γ*Tub-GFP;Dr/Tm6c* flies were used as a control. γ*Tub-GFP;Dhc64C*^{loa} mutant flies, containing a dominant loss-of-function F580Y point mutation in the dynein heavy chain, were provided by Dr. Simon Bullock of MRC labs in the United Kingdom. γ*Tub-GFP;Dhc64C*$^{8-1}$ mutant flies, containing a recessive hypomorphic mutation in the dynein heavy chain, were used also used. Dr. Simon Bullock's lab additionally provided two novel CRISPR mutants that disrupted a conserved DLIC binding site within the N-terminus of the *cen* coding sequence, γ*Tub-GFP;Cen*Δ12 and γ*Tub-GFP;Cen*Δ5. *Cen*Δ12 mutants consisted of an in-frame mutation that deleted 12 nucleotides of the conserved DLIC binding site. *Cen*Δ5 mutants consisted of an out-of-frame mutation that deleted 5 nucleotides of the conserved DLIC binding site. Flies were raised and maintained at 25°C in a light- and temperature-controlled chamber.

Construction of *cen* Transgenic Sequences

To generate HA-tagged *cen* transgenic constructs, the pENTR/TOPO plasmid backbone, with (+ATG) and without (-ATG) "sticky ends" corresponding to the translation start codon, was PCR amplified. Then, inserts of the *cen* coding sequence, with and without the translational start codon, were PCR amplified to generate overlapping "sticky ends". HA-tags were incorporated as pre-synthesized oligomers. Primers are listed in Table 1. pENTR backbones and *cen* inserts were ligated with Gibson Assembly using an 1:1:2 molar ratio of plasmid:*cen* cDNA:HA tag. Sequences were verified by DNA sequencing and were recombined into the *pPW-attB*

destination vector using the Gateway cloning system. *Drosophila* transgenesis was carried out by BestGene, Inc. Four independent isolates for -ATG and five independent isolates for +ATG were obtained per site-specific integration into the attP2 site on the third chromosome by PhiC31 integrase-mediated transgenesis.

Detection of RNA through smFISH

All smFISH protocols were performed with RNase-free solutions. Collected 0-2.5 hours embryos were rehydrated in 100% methanol (3:7, 1:1, 7:3) and PBST and then washed in WB* buffer and HB* buffer. Then, embryos were incubated in a 37°C water bath in *cen* probe diluted 1:50 in HB* buffer. smFISH probes were designed to bind to complementary RNA to make specific RNA fluorescent under the microscope. After the overnight water bath incubation, embryos were washed repeatedly in pre-warmed WB* buffer (15 minutes for three times). Then, embryos were stained with DAPI for 30 minutes, washed with PBST three times for five minutes each, and mounted with Vectashield mounting medium. Slides were stored at 4°C, avoiding light, and imaged within three days.

Microscopy

Images were captured on a Nikon Ti-E system fitted with Yokagawa CSU-X1 spinning disk head, Hamamatsu Orca Flash 4.0 v2 digital CMOS camera, Nikon LU-N4 solid state laser launch (15 mW 405, 488, 561, and 647 nm) using the following objectives: ×100, 1.49 NA Apo TIRF oil immersion objective. Images were acquired using a Vectashield medium.

Image Analysis

Images were adjusted using the FIJI program and Microsoft PowerPoint to separate or merge the channel, create the maximum intensity projection, adjust the brightness and contrast, and crop regions of interest.

Statistical Analysis

Statistical analyses were conducted using a Brown-Forsythe and Welch ANOVA followed by Dunnett's T3 multiple comparisons test (*, $P<0.05$; **, $P<0.005$; **** $P<0.0001$). Data were plotted and statistical analysis was performed using GraphPad Prism software. Data shown are representative results from at least 3 independent experiments (total $n \geq 30$), as indicated in the figure legends.

RNA Measurement and Detection

For quantification of single-molecule RNA distribution relative to centrosomes, single-channel .tif raw images were segmented in three dimensions using code adapted from the Allen Institute for Cell Science (Chen et al., 2018). Distances were measured from the surface of each RNA object to the surface of the closest centrosome. Single molecules of RNA are objects of 50–100 pixels, as determined by their diffraction-limited 200-nm size. For the *cen* RNA probe, we divided the integrated intensity of each RNA object by the averaged integrated intensity of all single-molecule RNAs, allowing an estimate of the number of RNA molecules per object. We then calculated the percentage of total RNA that overlapped with centrosomes. A detailed protocol for RNA analysis was previously described (Ryder and Lerit, 2020; Ryder et al., 2020).

Table 1: Primers and Oligomers

Primer	Description (5′ to 3′)
M13 Forward	GTAAAACGACGGCCAG
Cen N-term Seq	GTGGTCAGCGTCTTAATCTGC
Cen C-term Seq	ATCCTACGCCGAAGTTTTGC
	To check colony PCR of *cen* transgenic constructs and confirm presence of the -ATG deletion (Cen N-term Seq) as well as the HA tag (Cen C-term Seq).
C-term HA tag (oligomer)	GGCGGCAGCGGTGGAAGTGGTGGTAGTGGAGGAAGTTACCCATACGATGTTC CTGACTATGCGGGCTATCCCTATGACGTCCCGGACTATGCAGGATCCTATCCA TATGACGTTCCAGATTACGCTTAA
	To insert a hemagglutinin (HA) tag to each C-terminus of *cen* transgenic constructs.
pENTR BB Reverse (+ATG)	CCGTGATTGGATTCCTCG<u>ATG</u>GTGAAGGGGGCGGC
pENTR BB Reverse (-ATG)	CCGTGATTGGATTCCTCGGTGAAGGGGGCGGC
pENTR BB Forward	CCTATCCATATGACGTTCCAGATTACGCTTAAAAGGGTGGGCGCG
	To create pENTR backbone (BB) for *cen* transgenic constructs. Translational start codon underlined.
Cen cDNA Forward (+ATG)	CCGCGGCCGCCCCCTTCACC<u>ATG</u>GAGGAATCCAATCACGGTTC
Cen cDNA Forward (-ATG)	CCGCGGCCGCCCCCTTCACCGAGGAATCCAATCACGGTTC
Cen cDNA Reverse	TCCACCGCTGCCGCCCTTTTGACGAAACTGATGATGATGAC
	To amplify *cen* coding sequence for *cen* transgenic constructs. Translational start codon underlined.

References

Ambrose JC, Li W, Marcus A, Ma H, Cyr R. A minus-end-directed kinesin with plus-end tracking protein activity is involved in spindle morphogenesis. Mol Biol Cell. 2005 Apr;16(4):1584-92. doi: 10.1091/mbc.e04-10-0935.

Bergalet J, Patel D, Legendre F, et al. Inter-dependent Centrosomal Co-localization of the cen and ik2 cis-Natural Antisense mRNAs in Drosophila. *Cell Rep*. 2020;30(10):3339-3352.e6. doi:10.1016/j.celrep.2020.02.047

Blower MD. Molecular insights into intracellular RNA localization. Int Rev Cell Mol Biol. 2013;302:1-39. doi: 10.1016/B978-0-12-407699-0.00001-7.

Clark A, Meignin C, Davis I. A Dynein-dependent shortcut rapidly delivers axis determination transcripts into the Drosophila oocyte. Development. 2007 May;134(10):1955-65. doi: 10.1242/dev.02832.

Das S, Vera M, Gandin V, Singer RH, Tutucci E. Intracellular mRNA transport and localized translation. Nat Rev Mol Cell Biol. 2021 Jul;22(7):483-504. doi: 10.1038/s41580-021-00356-8. Erratum in: Nat Rev Mol Cell Biol.

Deng W, Garrett C, Dombert B, Soura V, Banks G, Fisher EM, van der Brug MP, Hafezparast M. Neurodegenerative mutation in cytoplasmic dynein alters its organization and dynein-dynactin and dynein-kinesin interactions. J Biol Chem. 2010 Dec 17;285(51):39922-34. doi: 10.1074/jbc.M110.178087.

Dionne LK, Shim K, Hoshi M, Cheng T, Wang J, Marthiens V, Knoten A, Basto R, Jain S, Mahjoub MR. Centrosome amplification disrupts renal development and causes cystogenesis. J Cell Biol. 2018 Jul 2;217(7):2485-2501. doi: 10.1083/jcb.201710019.

Eliscovich C, Buxbaum AR, Katz ZB, Singer RH. mRNA on the move: the road to its biological destiny. J Biol Chem. 2013 Jul 12;288(28):20361-8. doi: 10.1074/jbc.R113.452094.

Foe VE, Alberts BM. Studies of nuclear and cytoplasmic behaviour during the five mitotic cycles that precede gastrulation in Drosophila embryogenesis. J Cell Sci. 1983 May;61:31-70. doi: 10.1242/jcs.61.1.31.

Gepner J, Li M, Ludmann S, Kortas C, Boylan K, Iyadurai SJ, McGrail M, Hays TS. Cytoplasmic dynein function is essential in Drosophila melanogaster. Genetics. 1996 Mar;142(3):865-78. doi: 10.1093/genetics/142.3.865.

Gibson, D., Young, L., Chuang, RY. *et al.* 2009 Enzymatic assembly of DNA molecules up to several hundred kilobases. *Nat Methods* **6,** 343–345 https://doi.org/10.1038/nmeth.1318

Goodson HV, Jonasson EM. Microtubules and Microtubule-Associated Proteins. Cold Spring Harb Perspect Biol. 2018 Jun 1;10(6):a022608. doi: 10.1101/cshperspect.a022608.

Ilieva HS, Yamanaka K, Malkmus S, Kakinohana O, Yaksh T, Marsala M, Cleveland DW. Mutant dynein (Loa) triggers proprioceptive axon loss that extends survival only in the SOD1 ALS model with highest motor neuron death. Proc Natl Acad Sci U S A. 2008 Aug 26;105(34):12599-604. doi: 10.1073/pnas.0805422105.

Kelvinsong. “Centrosome - Definition and Examples - Biology Online Dictionary.” Biology Articles, Tutorials & Dictionary Online, 30 Aug. 2021, https://www.biologyonline.com/dictionary/centrosome.

Lécuyer E, Yoshida H, Parthasarathy N, Alm C, Babak T, Cerovina T, Hughes TR, Tomancak P, Krause HM. Global analysis of mRNA localization reveals a prominent role in organizing cellular architecture and function. Cell. 2007 Oct 5;131(1):174-87. doi: 10.1016/j.cell.2007.08.003.

Macdonald PM, Struhl G. cis-acting sequences responsible for anterior localization of bicoid mRNA in Drosophila embryos. Nature. 1988 Dec 8;336(6199):595-8. doi: 10.1038/336595a0.

Martin KC, Ephrussi A. mRNA localization: gene expression in the spatial dimension. Cell. 2009 Feb 20;136(4):719-30. doi: 10.1016/j.cell.2009.01.044.

Moritz M, Braunfeld MB, Sedat JW, Alberts B, Agard DA. Microtubule nucleation by gamma-tubulin-containing rings in the centrosome. Nature. 1995 Dec 7;378(6557):638-40. doi: 10.1038/378638a0.

Rappaport R. Experiments concerning the cleavage stimulus in sand dollar eggs. *J Exp Zool*. 1961;148:81-89. doi:10.1002/jez.1401480107

Ross JL, Shuman H, Holzbaur EL, Goldman YE. Kinesin and dynein-dynactin at intersecting microtubules: motor density affects dynein function. Biophys J. 2008 Apr 15;94(8):3115-25. doi: 10.1529/biophysj.107.120014.

Ryder PV, Fang J, Lerit DA. centrocortin RNA localization to centrosomes is regulated by FMRP and facilitates error-free mitosis. *J Cell Biol*. 2020;219(12):e202004101. doi:10.1083/jcb.202004101

Ryder PV, Lerit DA. Quantitative analysis of subcellular distributions with an open-source, object-based tool. Biol Open. 2020 Oct 19;9(10):bio055228. doi: 10.1242/bio.055228.

Setu, T. and Basak, T. (2021) An Introduction to Basic Statistical Models in Genetics. Open Journal of Statistics, 11, 1017-1025. doi: 10.4236/ojs.2021.116060.

Woodruff JB, Ferreira Gomes B, Widlund PO, Mahamid J, Honigmann A, Hyman AA. The Centrosome Is a Selective Condensate that Nucleates Microtubules by Concentrating Tubulin. Cell. 2017 Jun 1;169(6):1066-1077.e10. doi: 10.1016/j.cell.2017.05.028.

Woodruff JB, Wueseke O, Hyman AA. Pericentriolar material structure and dynamics. Philos Trans R Soc Lond B Biol Sci. 2014 Sep 5;369(1650):20130459. doi: 10.1098/rstb.2013.0459.

Xiang X, Qiu R. Cargo-Mediated Activation of Cytoplasmic Dynein in vivo. Front Cell Dev Biol. 2020 Oct 23;8:598952. doi: 10.3389/fcell.2020.598952.

Zein-Sabatto H, Lerit DA. The identification and functional analysis of mRNA localizing to centrosomes. Front Cell Dev Biol. 2021;9:782802.

Zhang L, Si Q, Yang K, Zhang W, Okita TW, Tian L. mRNA Localization to the Endoplasmic Reticulum in Plant Endosperm Cells. Int J Mol Sci. 2022 Nov 4;23(21):13511. doi: 10.3390/ijms232113511.